

Total cross sections for positron and electron collisions with NH_3 and H_2O molecules

O Sueoka, S Mori and Y Katayama†

Institute of Physics, College of Arts and Sciences, University of Tokyo, 3-8-1 Komaba, Meguro-ku, Tokyo 153, Japan

Received 16 September 1986, in final form 5 January 1987

Abstract. The total cross sections for 1–400 eV positrons and electrons colliding with NH_3 and H_2O molecules were measured using a TOF method. The cross sections were obtained by a normalisation method. The results for e^+-NH_3 and $\text{e}^+-\text{H}_2\text{O}$ at low energy were much lower than the theoretical values of Jain. The cross sections of positronium formation in these gases were measured.

1. Introduction

Electron collisions with NH_3 and H_2O molecules are of interest in atomic and molecular processes in chemical reactions, interstellar space, atmosphere and radioactive collisions. However, there have been few studies of electron collision processes in these gases. Moreover, no data for positron collisions have yet been presented. In this paper, measurements of positron and electron collisions with NH_3 molecules were performed using the same apparatus and experimental procedure, and the results were compared with those from water vapour studies, of which the main data were published in a preliminary report (Sueoka *et al* 1986). The data of the H_2O experiment have shown that the probability of positronium (Ps) formation is very low. One of the purposes of this paper is to determine whether these phenomena are also apparent in ammonia molecules, which are polar molecules (of polarisability 1.48 D), though the other aim is to provide the cross section data. For H_2O molecules, only supplementary measurements were carried out.

Recently, Jain (1986) has reported theoretical studies based on the fixed-nuclei approximation for positron scattering by H_2O and NH_3 molecules, in which the values of the total cross sections and the momentum transfer cross sections for positrons are given. The theoretical results for these polar molecules show extremely high values not only in the low-energy range (below 1 eV) but also in the range 1–3 eV.

Part of the present work for e^+-NH_3 has been reported elsewhere (Sueoka and Mori 1984a). The previous data for positron collisions were used in this paper, but those obtained at low energies were established in this experiment. The previous data for electrons were modified to new values obtained under improved conditions.

† Present address: Science Institute, IBM Japan Ltd, 5-19 Sanbancho, Chiyoda-ku, Tokyo 102, Japan.

2. Experimental method

The measurements of the total cross section were performed under the same experimental conditions as in the preliminary report of the study for H_2O molecules (Sueoka *et al* 1986).

2.1. Projectile particles

Radioactive ^{22}Na with an activity of about $50\ \mu\text{Ci}$ was used as a positron source, and ^{137}Cs with an activity of $40\ \mu\text{Ci}$ was used as an electron source. A set of annealed tungsten ribbons was used as a positron moderator (Dale *et al* 1980). The same tungsten ribbon was also used as an electron moderator. As examples, an electron beam profile with an acceleration energy of 0.1 eV using an axial magnetic field of 3 G and a positron beam profile of 0.2 eV in a field of 4.5 G, by which the projectile particles were transported in the flight path, are shown in figure 1. Small and fine structures in the spectra are affected by the magnetic field and the projectile energy in the present geometry. Typical numbers of slow electrons are 100 and $200\ \text{e}^- \text{s}^{-1}$ in the case of 3 and 4.5 G, respectively, at an acceleration energy of near 0 eV. For positron beams, the numbers are 2 and $6\ \text{e}^+ \text{s}^{-1}$ in the case of 4.5 and 9 G near 0 eV.

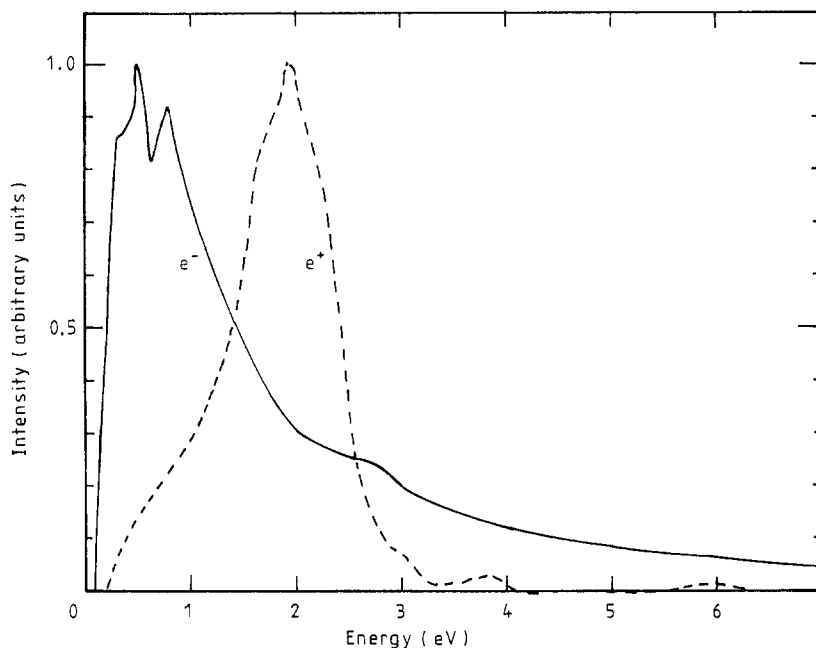


Figure 1. Electron beam profile for an acceleration energy of 0.1 eV at 3 G (full curve); positron beam profiles of 0.2 eV at 4.5 G (broken curve).

2.2. Apparatus and experimental procedure

The apparatus, electronics and methods of data analysis are nearly the same as those described in our previous paper (Sueoka and Mori 1986). A schematic diagram of the

experimental arrangement is shown in figure 2. The system of measurement was automatically operated. The gas pressure was accurately controlled using a fine controllable valve driven by a motor. A reservoir for water vapour was prepared, which was made of glass. For the ammonia molecule a stainless steel reservoir was used. Water vapour and ammonia are troublesome gases when working in a vacuum system. During the changeover from a gas run to a vacuum run, measurement was delayed for 220 s because of the difficulty in evacuating the target gases.

The magnetic field dependence of the cross section was checked for electron collisions with NH_3 as shown in figure 3. The dependence is almost the same as that

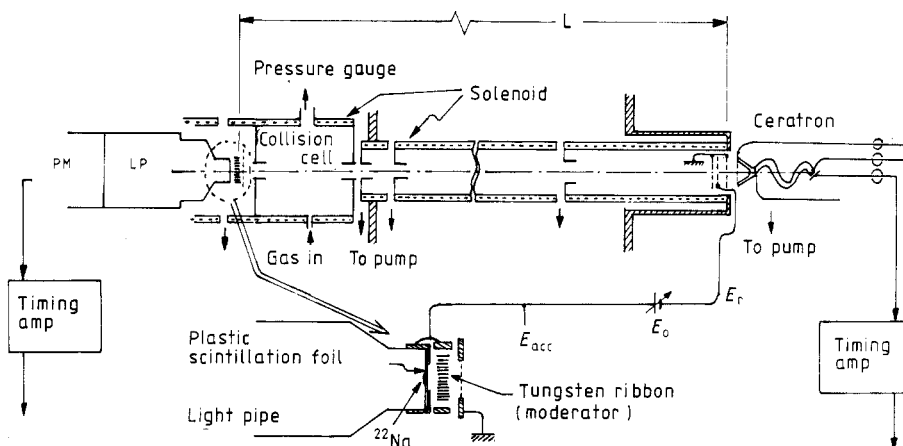


Figure 2. Schematic diagram of the experimental arrangement. The actual length of the collision cell is 52.5 mm. PM and LP indicate the photomultiplier and the light pipe, respectively.

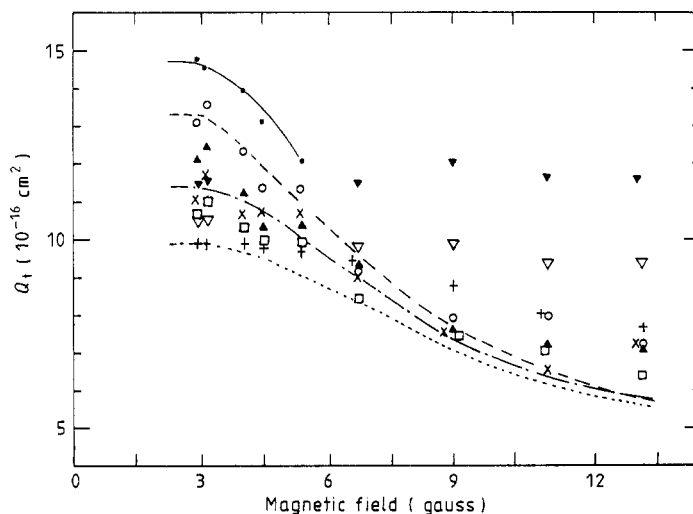


Figure 3. Total cross sections for electrons with NH_3 plotted against the magnetic field. \circ , 1.0 eV; \triangle , 1.2 eV; \blacktriangle , 1.4 eV; \times , 1.6 eV; \square , 2.0 eV; $+$, 2.5 eV; ∇ , 3.1 eV; \blacktriangledown , 4.0 eV. The curves are the data for H_2O of the previous work (Sueoka *et al* 1986) which are modified to visual fitted curves and are normalised to the values for NH_3 at 3 G. (—), 1.0 eV; (---), 1.2 eV; (— · —), 1.6 eV; (----), 2.0 eV.

in e^- -H₂O (Sueoka *et al* 1986), for low energies of 1.0–1.4 eV, suggesting a sharp forward-peaked scattering, but that for higher energies is very different from that in e^- -H₂O. Because the cross sections in the magnetic field used were almost saturated, as shown in figure 3, the cross sections for electrons were little affected by the effect of the magnetic field except at the lowest energy. For positron collision experiments, the weaker magnetic field (4.5 G) was applied only for the range below 6.5 eV. Although measurements in the weaker field may be necessary in the range below 2 eV, they were not performed because of the resulting extremely weak beam intensity.

In order to ensure the independence of the effective length of the collision cell on cell pressure, the measurements for the electron collision were performed for H₂O and NH₃ molecules. As shown in figure 4, a slight dependence on the gas pressure was apparent perhaps because of the short length of the collision cell. However, this slight dependence gives rise to less than a 2% higher error in the total cross section in the high cross section value measurements.

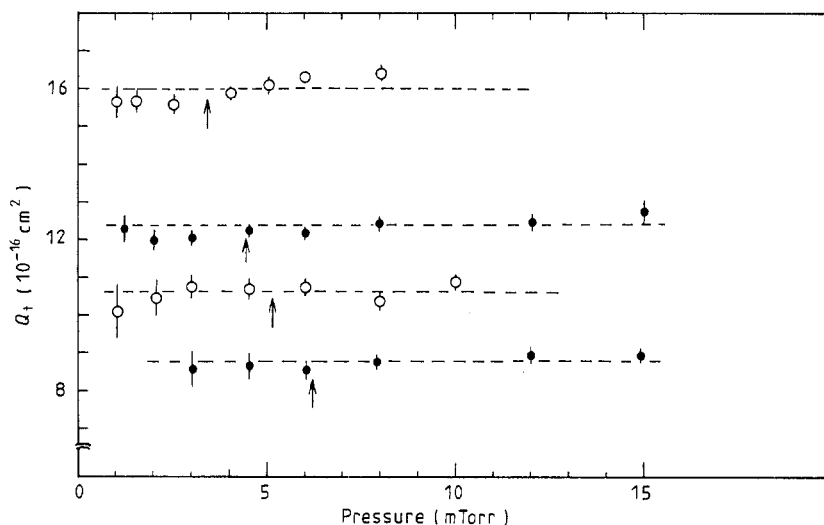


Figure 4. Total cross sections plotted against gas pressure. \circ , for e^- -NH₃; \bullet , for e^- -H₂O. Error bars show only the statistical error. The arrows indicate the pressure at a beam-intensity attenuation (I_v/I_i) of 3. Top two plots at 6.7 eV, bottom two plots at 33.5 eV.

A retarding potential method based on TOF spectroscopy was applied for eliminating the contribution of large energy-loss inelastic scattering and for decreasing forward-scattered contributions with reduced axial velocities. The retarding potential (E_r) was the same as the acceleration potential (E_{acc}) for electron collisions, and E_r was equal to or 1.5 eV lower than E_{acc} for positron collisions. The effect of the retarding potential on the TOF spectrum was corrected to give the conventional TOF spectrum in which the retarding potential was not applied. The low-energy parts of the spectrum were not used as data, because the data in these channels included the signal of scattered particles.

The energy scale for electron collision measurements was calibrated by the shape resonance of electron scattering by CO₂ and N₂ molecules. The calibration for positrons was not performed. A detailed discussion was presented in the previous paper (Sueoka and Mori 1986).

2.3. Data collection

The true signal spectrum was computed from raw TOF data by the method of Coleman *et al* (1974). The total cross section Q_t is given as follows:

$$Q_t = (1/\rho l) \ln(I_v/I_g)$$

where ρ is the gas number density in the collision cell; l is the effective length of the cell which was derived by normalisation of the total cross sections in e^+-N_2 in the energy range 25–400 eV to the data of Hoffman *et al* (1982), i.e. the total cross section was obtained relatively; I_v and I_g are net counts differing by the accidental coincidence in the vacuum and in the gas run. The normalisation procedure was carried out anew for the current measurements.

2.4. Error estimation

The error was estimated by addition of $\Delta\rho/\rho$, $\Delta l/l$ and $\Delta I/I$, where I means $\ln(I_v/I_g)$. ΔI includes all statistical errors in the counting. The value of $\Delta I/I$ for positron collisions is 2–3% for the range above 10 eV and 3–5% below 9.5 eV. This kind of error for electron collisions is about 1%. For the weaker magnetic field measurements at the low energy range, statistical errors are larger. The error in the gas density $\Delta\rho$ is almost certainly due to the resolution of a Baratron gauge (0.1 mTorr); $\Delta\rho/\rho$ is 1.5–6% depending on the colliding gas pressure. As the temperature of the target gas was automatically recorded and the gas pressure was controlled by a microcomputer, the error caused by these fluctuations was negligible. The error due to the normalisation procedure for the determination of the effective length $\Delta l/l$ was estimated to be about 3% and was counted as the error of ΔI including systematic uncertainties estimated by reproducibility of independent measurements. The systematic uncertainties due to forward scattering and the error in the data for e^+-N_2 of Hoffman *et al* (1982) used in the normalisation were not counted in the present paper.

3. Results and discussion

3.1. e^+-NH_3 and e^+-H_2O

The total cross sections for positrons colliding with NH_3 were obtained using a magnetic field of 4.5 G in the range 1–7.5 eV, of 9 G in the range 0.7–400 eV. In the 4–7.5 eV range, the data of the two magnetic field conditions merge. The present data in the range below 20 eV are shown in figure 5 together with the experimental data for H_2O molecules of Sueoka *et al* (1986) and the theoretical values for H_2O and NH_3 of Jain (1985). Similarities between the cross section curve of NH_3 and that of H_2O for positron collisions are shown in all energy ranges. The theoretical values in the range below 3 eV are about four times the present experimental data for NH_3 and about five times those for H_2O . Taking into consideration the results in figures 3 and 5, it is deduced that our results are not so strongly suppressed by forward scattering. In particular, for NH_3 , underestimation of the total cross section due to this effect may not be significant in our results. On the other hand, our experimental values largely differ from Jain's theoretical values. The theoretical calculation was based on the fixed-nuclei approximation in which the optical potential consists of a static term obtained from

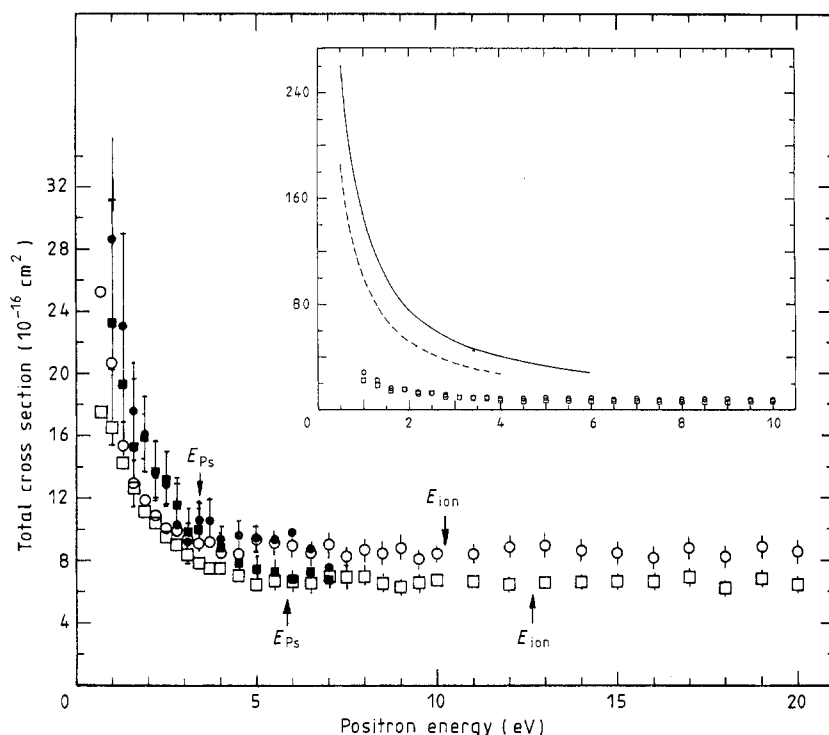


Figure 5. Total cross sections for 1–20 eV positrons colliding with NH_3 and H_2O . \circ , 9 G, \bullet , 4.5 G with NH_3 ; \square , 9 G, \blacksquare , 4.5 G with H_2O . In the inset, the full and the broken curves show the theoretical values of Jain (1985) for H_2O and NH_3 , respectively; \square and \circ show the present data for H_2O and NH_3 . The threshold energies of positronium formation and ionisation are shown by arrows.

the near-Hartree-Fock single centre target wavefunctions and a parameter-free polarisation term. Jain also gave the theoretical values based on the Born approximation by which the values were about 3.5 times the experimental data for NH_3 . The experimental data of Sueoka and Mori (1984a, b) cited in Jain's paper are the 9 G measurement data for electrons and positrons. Although the present data are an improvement, a large discrepancy still remains as shown in figure 5.

The Ps formation cross sections were obtained by the method of Stein and Kaupilla (1982). In the data at 4.5 and 9 G for e^+-NH_3 and $\text{e}^+-\text{H}_2\text{O}$ of Sueoka *et al* (1986), the Ps formation cross sections were less than $1 \times 10^{-16} \text{ cm}^2$ at a few eV above the threshold energy of positronium formation (E_{Ps}). An improved experiment, using a stronger magnetic field of 23 G, was performed. The results were $(0.9 \pm 0.4) \times 10^{-16} \text{ cm}^2$ for NH_3 at $E_{\text{Ps}} + 2 \text{ eV}$ (at 5.4 eV), $(0.3 \pm 0.2) \times 10^{-16} \text{ cm}^2$ for H_2O at $E_{\text{Ps}} + 2 \text{ eV}$ (at 7.8 eV).

In any case, these values are fairly low in comparison with those for many other non-polar molecules. This phenomenon is also shown in the Z_{eff} parameter which is the effective number of annihilation electrons of the NH_3 molecule taking into account the effect of polarisation of the molecule due to the projectile positrons. The theory of Jain and Thompson (1983a) has shown that the Z_{eff} value for NH_3 molecules is one order larger than that for CH_4 . As pointed out by Goldanskii (1968), the probability of positronium formation in a polar molecule is low because a strong dipole field with increasing localisation of negative electric charge is induced by a positron. For such

an effect to be realised, the electron density around a positron must be locally enhanced to a high value as in a metal. It was shown that even in the lowest electron density metal, no positronium is formed (Kanazawa *et al* 1965).

3.2. e^- - NH_3 and e^- - H_2O

The total cross sections for electrons colliding with NH_3 molecules in the range 1–400 eV were measured using a magnetic field of 4.5 and 3 G in the range 1–10 eV. The data at 4.5 and 3 G merge within the statistical errors in the range 1.8–10 eV. Considering the accuracy of the data, the results at 4.5 G in the 2.2–400 eV range and those at 3 G in the 1.0–2.0 eV range are adopted as the total cross section values of the present measurement. The present data are shown in figure 6 together with the experimental data for H_2O of Sueoka *et al* (1986), Brüche's (1929) data for NH_3 and the theoretical data (multiplied by a factor of $\frac{1}{3}$) of Jain and Thompson (1983b) which are the integrated cross sections for the $00 \rightarrow 10$ rotation excitation in H_2O molecules. In the range below 3 eV, the $\frac{1}{3}$ plot of the theoretical data fits the experimental data well. The total cross sections for electrons with NH_3 are not high even in the low-energy range, while those for H_2O increase fairly sharply with decreasing impact energy. Moreover, the dependence of the magnetic field in which the scattering is forward-peaked is revealed only in the range below 1.6 eV for NH_3 , while the difference for each magnetic field is fairly large for the H_2O data. These phenomena are explained by figure 2 and figure 1 of the previous report (Sueoka *et al* 1986). As NH_3 and H_2O molecules are typical polar

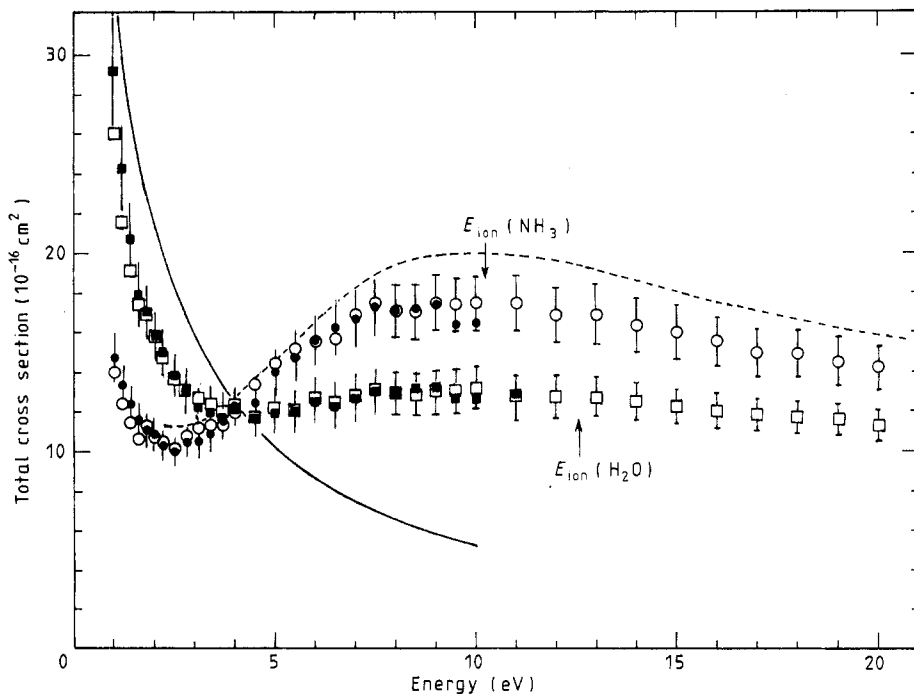


Figure 6. Total cross sections for 1–20 eV electrons colliding with NH_3 and H_2O . \circ , 4.5 G, \bullet , 3 G with NH_3 ; (---), Brüche's experimental data with NH_3 ; \square , 4.5 G, \blacksquare , 3 G with H_2O . The full curve gives the theoretical data for e^- - H_2O of Jain and Thompson (1983b) multiplied by a factor of $\frac{1}{3}$. The threshold energy of ionisation E_{ion} is shown by an arrow.

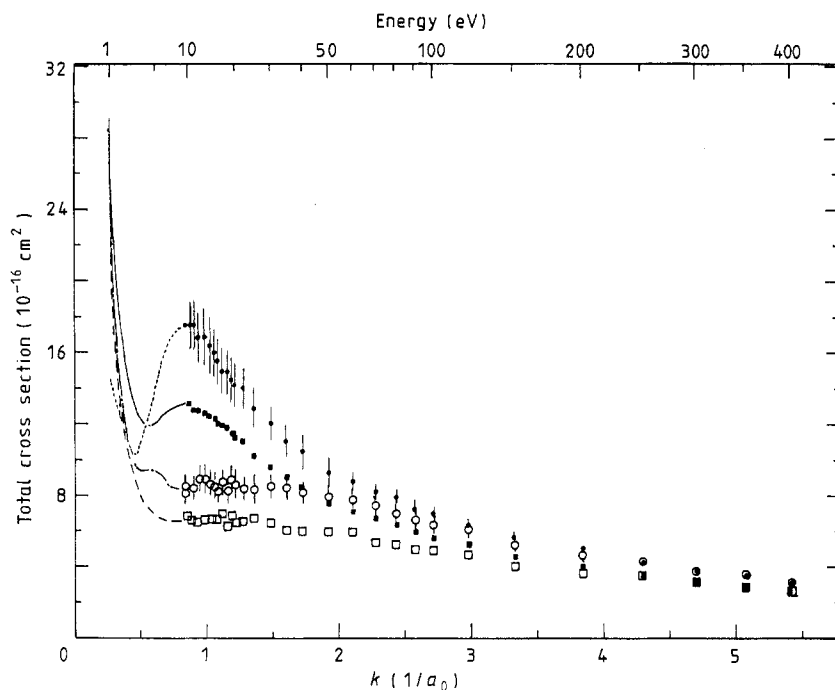


Figure 7. Total cross sections for positrons and electrons plotted against wavenumber k extending to intermediate energies. \circ , (---), for e^+ - NH_3 with errors; \square , (---), for e^+ - H_2O ; \bullet , (----), for e^- - NH_3 with errors; \blacksquare , (—), for e^- - H_2O . The data below 10 eV are modified to the lines of visually fitted curves.

molecules, very high values of the cross section due to rotational excitations in the low-energy range are expected (Itikawa 1978). However, the data for NH_3 are not high, but are in fact rather low. The cross section may be largely increased in the low-energy range below 1 eV, and measurements in this range are expected. There are no total cross section calculations available for comparison.

On the other hand, the results shown in figure 3 suggest that in the differential cross section data for e^- - NH_3 a drastic difference is expected for impact energies of 1 and 5 eV. Brüche's data are considerably higher than the present values, as are the data of other electron measurements such as those for hydrocarbons (Sueoka and Mori 1986). The cross section curve for NH_3 has a minimum $Q_{\min}^- = 10 \times 10^{-16} \text{ cm}^2$ at 2.5 eV and a maximum $Q_{\max}^- = 17.2 \times 10^{-16} \text{ cm}^2$ at 9 eV, while the minimum and the maximum in the curve for H_2O are inconspicuous.

3.3. e^\pm - NH_3 and e^\pm - H_2O in the intermediate-energy range

The total cross sections for positrons and electrons in the range between 1 and 400 eV are plotted against the wavenumber k in figure 7. In the intermediate-energy range, the curves of total cross sections of H_2O and NH_3 molecules also present a similar tendency for electron and positron scatterings. In the range above 250 eV the data almost coincide with each other.

The values for NH_3 of the total cross section for positrons are given in table 1; those for electrons are given in table 2. The indicated error was obtained by the

Table 1. Total cross sections for positron collisions (10^{-16} cm^2) for NH_3 . The cross section values in the range 1.0–4.5 eV are taken from the 4.5 G measurement, and the others are taken from the 9 G measurement.

| Energy (eV) | Cross section | Energy (eV) | Cross section |
|-------------|----------------|-------------|---------------|
| 1.0 | 28.7 ± 8.5 | 14.0 | 8.7 ± 0.8 |
| 1.3 | 23.1 ± 6.2 | 15.0 | 8.5 ± 0.7 |
| 1.6 | 17.6 ± 3.2 | 16.0 | 8.2 ± 0.8 |
| 1.9 | 16.0 ± 2.5 | 17.0 | 8.8 ± 0.7 |
| 2.2 | 13.7 ± 1.8 | 18.0 | 8.3 ± 0.8 |
| 2.5 | 12.9 ± 1.7 | 19.0 | 8.9 ± 0.8 |
| 2.8 | 10.3 ± 1.5 | 20.0 | 8.6 ± 0.8 |
| 3.1 | 9.3 ± 1.4 | 22.0 | 8.4 ± 0.7 |
| 3.4 | 10.6 ± 1.3 | 25.0 | 8.3 ± 0.7 |
| 3.7 | 10.5 ± 1.2 | 30.0 | 8.5 ± 0.7 |
| 4.0 | 9.4 ± 0.9 | 35.0 | 8.4 ± 0.7 |
| 4.5 | 9.6 ± 1.0 | 40.0 | 8.2 ± 0.6 |
| 5.0 | 9.5 ± 0.9 | 50.0 | 7.9 ± 0.5 |
| 5.5 | 9.2 ± 0.8 | 60.0 | 7.7 ± 0.6 |
| 6.0 | 9.0 ± 0.8 | 70.0 | 7.4 ± 0.6 |
| 6.5 | 8.5 ± 0.8 | 80.0 | 7.0 ± 0.5 |
| 7.0 | 9.1 ± 0.8 | 90.0 | 6.6 ± 0.5 |
| 7.5 | 8.3 ± 0.9 | 100 | 6.3 ± 0.4 |
| 8.0 | 8.7 ± 0.8 | 120 | 6.0 ± 0.4 |
| 8.5 | 8.5 ± 0.7 | 150 | 5.2 ± 0.4 |
| 9.0 | 8.8 ± 0.7 | 200 | 4.6 ± 0.4 |
| 9.5 | 8.1 ± 0.7 | 250 | 4.3 ± 0.3 |
| 10.0 | 8.5 ± 0.6 | 300 | 3.8 ± 0.3 |
| 11.0 | 8.4 ± 0.7 | 350 | 3.5 ± 0.3 |
| 12.0 | 8.9 ± 0.7 | 400 | 2.7 ± 0.2 |
| 13.0 | 9.0 ± 0.8 | | |

Table 2. Total cross sections for electron collisions (10^{-16} cm^2) for NH_3 . The cross section values in the range 1.0–2.0 eV are taken from the 3 G measurement, and the others are taken from the 4.5 G measurement.

| Energy (eV) | Cross section | Energy (eV) | Cross section |
|-------------|----------------|-------------|----------------|
| 1.0 | 14.7 ± 1.3 | 6.0 | 15.5 ± 1.3 |
| 1.2 | 13.4 ± 1.1 | 6.5 | 15.7 ± 1.4 |
| 1.4 | 12.4 ± 1.0 | 7.0 | 16.9 ± 1.4 |
| 1.6 | 11.6 ± 0.9 | 7.5 | 17.5 ± 1.4 |
| 1.8 | 11.1 ± 0.9 | 8.0 | 17.1 ± 1.4 |
| 2.0 | 10.9 ± 0.9 | 8.5 | 17.1 ± 1.5 |
| 2.2 | 10.4 ± 0.8 | 9.0 | 17.5 ± 1.5 |
| 2.5 | 10.1 ± 0.8 | 9.5 | 17.5 ± 1.5 |
| 2.8 | 10.8 ± 0.8 | 10.0 | 17.5 ± 1.5 |
| 3.1 | 11.2 ± 0.9 | 11.0 | 17.5 ± 1.7 |
| 3.4 | 11.3 ± 0.9 | 12.0 | 16.9 ± 1.6 |
| 3.7 | 11.3 ± 1.0 | 13.0 | 16.9 ± 1.6 |
| 4.0 | 12.0 ± 1.0 | 14.0 | 16.4 ± 1.6 |
| 4.5 | 13.4 ± 1.2 | 15.0 | 16.0 ± 1.5 |
| 5.0 | 14.5 ± 1.2 | 16.0 | 15.5 ± 1.4 |
| 5.5 | 15.2 ± 1.3 | 17.0 | 15.0 ± 1.3 |

Table 2. (continued)

| Energy (eV) | Cross section | Energy (eV) | Cross section |
|-------------|----------------|-------------|---------------|
| 18.0 | 14.9 ± 1.3 | 80.0 | 7.9 ± 0.5 |
| 19.0 | 14.5 ± 1.3 | 90.0 | 7.3 ± 0.5 |
| 20.0 | 14.2 ± 1.3 | 100 | 7.0 ± 0.4 |
| 22.0 | 14.0 ± 1.1 | 120 | 6.3 ± 0.4 |
| 25.0 | 12.9 ± 1.1 | 150 | 5.6 ± 0.3 |
| 30.0 | 12.1 ± 1.0 | 200 | 5.0 ± 0.3 |
| 35.0 | 11.0 ± 1.0 | 250 | 4.2 ± 0.2 |
| 40.0 | 10.5 ± 1.0 | 300 | 3.9 ± 0.2 |
| 50.0 | 9.3 ± 0.9 | 350 | 3.5 ± 0.2 |
| 60.0 | 8.8 ± 0.6 | 400 | 3.2 ± 0.2 |
| 70.0 | 8.3 ± 0.5 | | |

addition of $\Delta I/I$, $\Delta\rho/\rho$ and $\Delta l/l$, not including the systematic errors due to forward scattering and the experimental error in the measurement of Hoffman *et al* (1982) used in the normalisation.

References

- Brüche E 1929 *Ann. Phys., Lpz.* **1** 93-134
 Coleman P G, Griffith T G and Heyland G R 1974 *Appl. Phys.* **5** 223-30
 Dale J M, Hulett L D and Pendyala S 1980 *Surf. Interface Anal.* **2** 199-203
 Goldanskii V I 1968 *At. Energ. Rev.* **6** 3-148
 Hoffman K R, Dababneh M S, Hsieh Y-F, Kauppila W E, Pol V, Smart J H and Stein T S 1982 *Phys. Rev. A* **25** 1393-403
 Itikawa Y 1978 *Phys. Rep.* **46** 117-64
 Jain A 1986 *3rd Int. Workshop on Positron (Electron)-Gas Scattering (Detroit)* ed W E Kauppila, T S Stein and J M Wadehra (Singapore: World Scientific)
 Jain A and Thompson D J 1983a *J. Phys. B: At. Mol. Phys.* **16** 1113-23
 — 1983b *J. Phys. B: At. Mol. Phys.* **16** 3077-98
 Kanazawa H, Ohtsuki Y H and Yanagawa S 1965 *Phys. Rev.* **138** A1155-57
 Stein T S and Kauppila W E 1982 *Adv. At. Mol. Phys.* **18** 53-96
 Sueoka O and Mori S 1984a *At. Coll. Res. Japan* **10** 17-8
 — 1984b *J. Phys. Soc. Japan* **53** 2491-500
 — 1986 *J. Phys. B: At. Mol. Phys.* **19** 4035-50
 Sueoka O, Mori S and Katayama Y 1986 *J. Phys. B: At. Mol. Phys.* **19** L373-78